Int. J. Electrochem. Sci., 13 **(2018)** 3745 – 3756, doi: 10.20964/2018.04.52

International Journal of
ELECTROCHEMICAL
SCIENCE
www.electrochemsci.org

Electrodeposited PbO_2 Thin Films with Different Surface Structure as Positive Plate in Lead Acid Batteries

Xuan Zhao, Cheng Li, Yaqiong Wang and Wenlin Xu[*]

College of Chemistry and Chemical Engineering, Yangzhou University, Yangzhou 225002, PR China.
[*]E-mail: wlxu@mail.yzu.edu.cn

Received: 17 December 2017 / *Accepted:* 5 February 2018 / *Published:* 6 March 2018

PbO_2 thin film is essential for applications in lead acid batteries system. In this work, PbO_2 thin films with different surface microstructure were fabricated through electrodeposition technique by controlling the deposition current density. Though PbO_2 thin films with porous structure are achieved at a high electrodeposition current density, the softening and leaching of the active materials on the electrode leads to a bad cycling charge-discharge ability. PbO_2 thin film fabricated at a low current density(PbO_2-20) has a compact and dense surface, and an activation process is needed to reach its maximum discharge ability with an improved cycling charge-discharge ability. Meanwhile, a porous structure is formed due to the active material expansion-contraction process, and then the discharge capacity is gradually reduced as observed in PbO_2 thin films obtained at high current density. Specifically, when PbO_2-20 film is assembled in a laboratory battery, the cycle charge-discharge life is 553 times at 1C with 30% depth of discharge much higher than that of PbO_2 thin film electrodeposited at a high current density.

Keywords: PbO_2 thin film; electrodeposition; lead acid battery; discharge capacity

1. INTRODUCTION

Advanced lead acid battery as one of the commercial power supply devices in electrochemical energy storage system faces a competition environmental from other kinds of energy sources. However, the high safety and low cost with reliable power performance make it still rank out for quite lots of applications such as hybrid electric vehicles, start/stop automotive systems, remote area power supply systems, renewable energy and grid storage applications and so on[1-5]. Such a lead acid battery consists of a number of plates, in the form of pasted grids which is manufactured by applying a paste to a lead grid. There are of course positive and negative plates in the batteries, and a paste is applied to the grid, and the plates are then subjected to an operation known as forming to convert the paste either to lead dioxide, in the case of a positive plate, or to spongy lead in the case of a negative plate. Generally, the capacity and cycle life of lead acid battery is restricted by the positive plate, thus positive plates have been received great efforts in order to improve the power performance [5-7].

Thin film electrodeposition that can form PbO_2 film onto Ti substrate from aqueous solution containing Pb^{2+} ion was considered as a promising approach to fabricate the electrode materials for energy storage system[8-16]. For example, PbO_2 thin film with porous structure used in lead-carbon super battery was prepared with a specific energy of 35.1 Wh kg^{-1} at 4C rate[10]. Dan et al. reported the Mn_3O_4-PbO_2 and SnO_2-PbO_2 composite material for supercapacitor, and these composite materials delivered a specific capacity of 338 F g^{-1} and 208 F g^{-1} in 1 M H_2SO_4 at 50mA cm^{-2}, respectively[12, 13]. A three-dimension porous Ti as substrate for PbO_2 electrode was fabricated by electrodeposition approach and discharge capacity of 132mAh g^{-1} in 1 M H_2SO_4 electrolyte with 900mA g^{-1} at a three-electrode system was reported [15]. In general, these previous relevant studies showed that PbO_2 thin film will be a promising candidate as positive electrode for lead acid batteries. Moreover, the structure with high porosity can undoubtedly facilitate the diffusion of HSO_4^- ion into the inner PbO_2 film which makes it easier for the reduction of PbO_2 to $PbSO_4$, and then increases the positive active material utilization[10, 14, 15]. However, the convert between $PbSO_4$ and PbO_2 is a complicated process, which involves change not only in microstructure but also phase compositions[17-19]. Thus, the investigation of electrochemical behavior of PbO_2 thin films with different initial morphologies and phase contents is a critical issue for a lead acid battery system.

Herein, we successfully prepared PbO_2 thin films with different surface sturcture onto a flat Ti/Sb-SnO_2 substrate by simply controlling the deposition time via electrodeposition approach. The surface morphology and phase composition of the thin films were characterized by field emission scanning electron microscope (FESEM), X-ray power diffraction (XRD) and thermogravimetric analysis (TGA). The electrochemical behaviors were investigated by electrochemical impedance spectroscopy (EIS) and galvanostatic charge-discharge (GCD) in 1 M H_2SO_4 electrolyte at a three-electrode system. For all the electrodeposited PbO_2 thin film, the discharge capacity increased with the increasing of cycling numbers, but gradually decreased when these films reached its maximum discharge capacity values. Though thin films electrodeposited at high current density with porous structure facilitated the charge and electrons transfer, the softening and leaching of the active materials resulted in a bad charge-discharge behavior. For the thin films electrodeposited at a low current density, namely PbO_2-20, had a relative lower initial discharge capacity but exhibited a much longer cycle life of discharge. When PbO_2-20 film was assembled in a laboratory battery, the cycle charge-discharge life is 553 times at 1C with 30% depth of discharge much higher than that of PbO_2 thin film electrodeposited at a high current density.

2. EXPERIMENTAL

2.1 Preparation of PbO_2 thin films

Ti/Sb-SnO_2 electrode was prepared according to the reports in Refs[9, 20], the sub-layer Sb-SnO_2 could avoid the formation of TiO_2 on the Ti surface. The Ti/Sb-SnO_2 electrode and lead plate were used as anode (9 cm^2) and cathode (12 cm^2), respectively, and Hg/Hg_2SO_4 electrode used as reference electrode consist of a conventional three-electrode cell. PbO_2 thin film was electrodeposited on Ti/Sb-SnO_2 electrode in an aqueous solution containing 0.5 M $Pb(NO_3)_2$ at a current density of 20 mA cm^{-2}, 70 mA cm^{-2} and 120 mA cm^{-2} respectively with a total given charge of 18C cm^{-2}. After that, the film was washed extensively with distilled water, and then dried at 80℃overnight. For convenience, the obtained films denoted as PbO_2-X, where X represent the current density of 20 mA cm^{-2}, 70 mA cm^{-2} and 120 mA cm^{-2}, respectively. All chemicals used in this experiment were AR grade and electrodeposition was performed on electrochemical work station (CHI660E Amp Booster, ChenHua, ShangHai, China) at 25 ^{o}C. The mass of the active material was determined by mass change of the substrate after deposition using electronic balance (FA2004B, ±0.1mg, TianMei, ShangHai, China).

2.2 Electrochemical measurements and physical characterization

Electrochemical performance was investigated in the above mentioned three-electrode cell, note that the as-prepared PbO_2 thin film was used as working electrode. Galvanostatic charge-discharge (GCD) curves were obtained using electrochemical workstation. Electrochemical impedance spectroscopy (EIS) was carried out on AutoLab-PGSTAT30 (Netherlands). EIS was performed within frequency range from 10000 Hz to 0. 1 Hz with 5 mV amplitude at 0.9 V (at the potential where the reduction reaction of PbO_2 to $PbSO_4$ occurred). GCD was conducted at 250 mA g^{-1} with cut-off potential of 0.6 V and then charged to potential of 1.4 V.

Battery tests were performed on battery test equipment (Newear 5V3A, ShenZhen, China) in a 5 M H_2SO_4 electrolyte at a constant temperature of 30 ^{o}C, after PbO_2 thin film was assembled as positive plate in a laboratory battery using a commercial negative plate and AGM separator (provided by Huafu Energy Storage Company, Jiangsu, China). The negative plate having a weight of 20 ± 0.5 g active mass and the electrodeposited PbO_2 thin film with a theory weight of 0.201g, thus the positive plate was really determining the performances of the battery. The discharge capacity for the laboratory battery was tested at different discharge rate of 0.1C, 0.5C, 1C, 3C and 5C, where the cut-off potential was set as 1.75V (100% depth of discharge 100% DOD) and charged at 1C rate until the battery reaches potential of 2.45V. The cycle life tests of these thin films were evaluated at a 30% DOD cycles with 1C rate, when the end potential of discharge below 1.75V the films could be considered as end of the cycle life.

The as-prepared thin films were characterized by X-ray powder diffraction (XRD; Bruker, D8 Advance, Germany; Cu Kα , λ=1.5418 Å, recorded from 10°~80°), Thermogravimetric Analysis (TGA; PerkinElmer Corporation, Pyris 1, American) and field emission scanning electronic microscopy(FESEM; Hitachi Limited Corporation, S-4800 II, Japan; 10kV).

3. RESULTS AND DISCUSSION

The surface morphology of PbO_2 thin films electrodeposited at different current density was observed by FESEM (Fig.1). The surface for PbO_2-20 thin film was dense and flat with pyramidal bumped agglomerates. However, the morphology was changed dramatically at a high current density. For PbO_2-70 thin film, a porous structure composed of microsphere grains was observed, and grains became further smaller in the case of PbO_2-120.

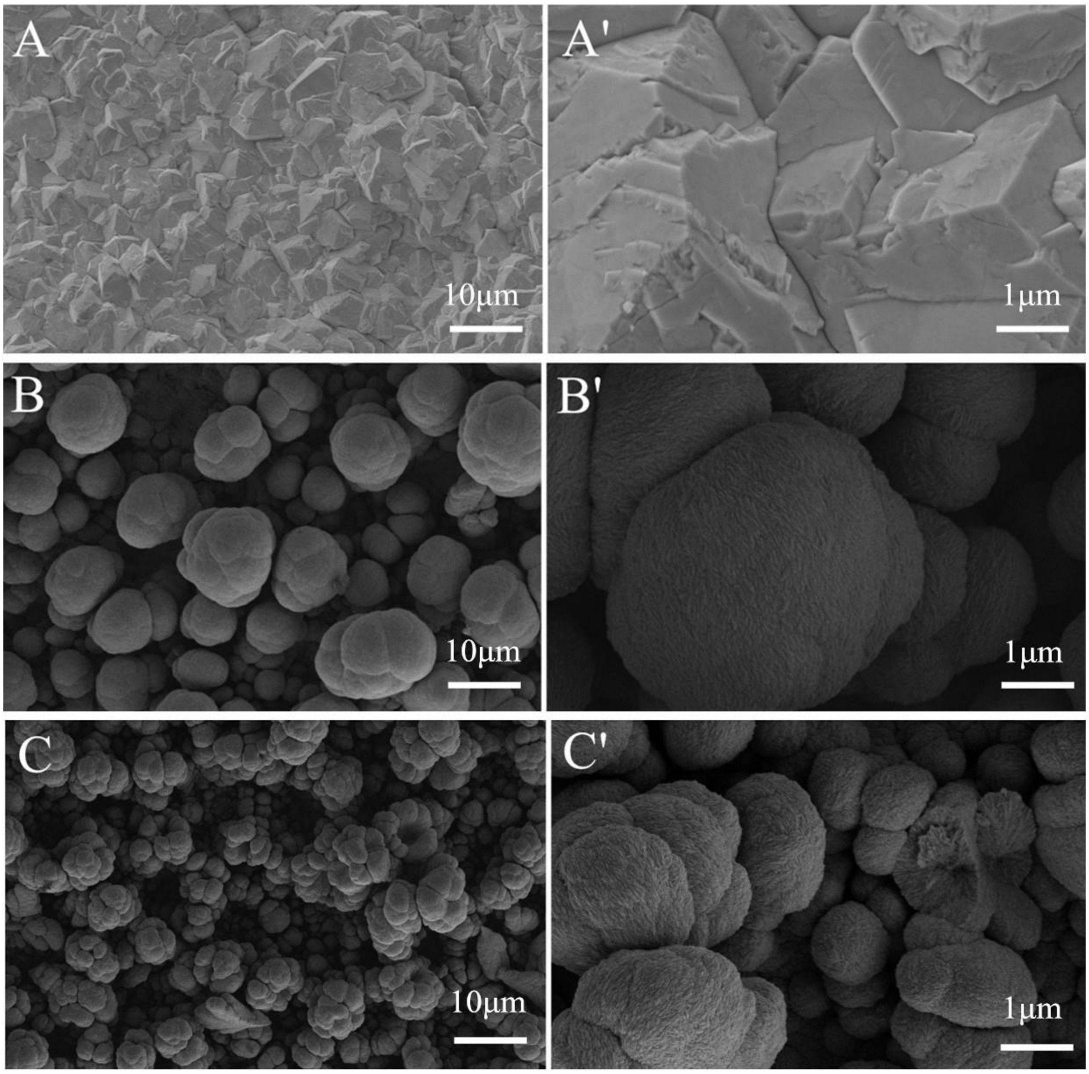

Figure 1. FESEM images of PbO_2 thin films prepared at different current density: PbO_2-20(A-A'), PbO_2-70(B-B'), PbO_2-120(C-C').

The reason for this significantly change in microstructure was related to the oxygen evolution reaction[9]. The nucleation and growth process for PbO_2 film was accompanied by oxygen evolution reaction, which plays a crucial role on the surface morphology formation during the deposition process[9]. Fig.2 shows the deposition potential as a function of deposition charge of PbO_2 thin films prepared at different current density. As show in Fig.2, the potential for formation of PbO_2-20 thin film was around 1.12 V, thus most of the charge contributed to the deposition of PbO_2 thin film. Without the effect of oxygen gas, the deposited layer exhibited a flat and dense surface. However, the potential for formation of PbO_2-70 and PbO_2-120 thin films was at potential of 1.33V and 1.59V, respectively.

Those potentials were accompanied by the formation of oxygen gas, a porous structure of PbO_2 thin films was observed at the high electrodeposited current [21, 22].

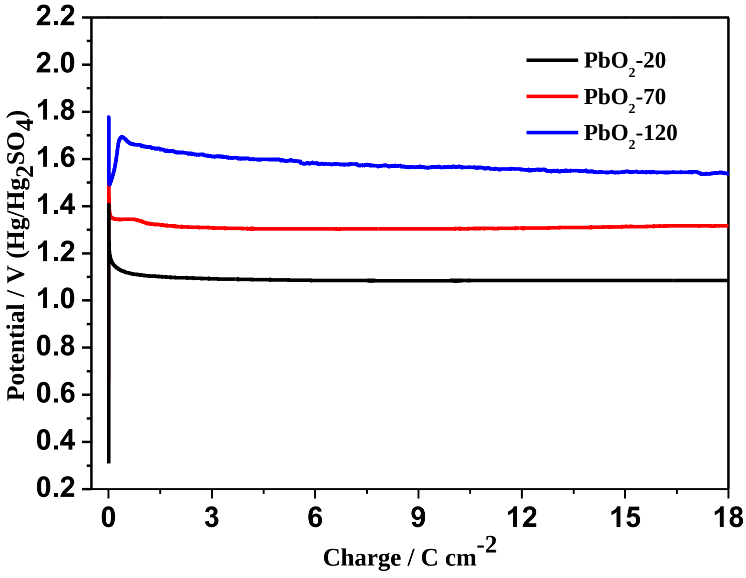

Figure 2. Potential vs. charge curves of PbO_2 thin films fabricated by electrodeposition at different current density in 0.5M $Pb(NO_3)_2$ solution.

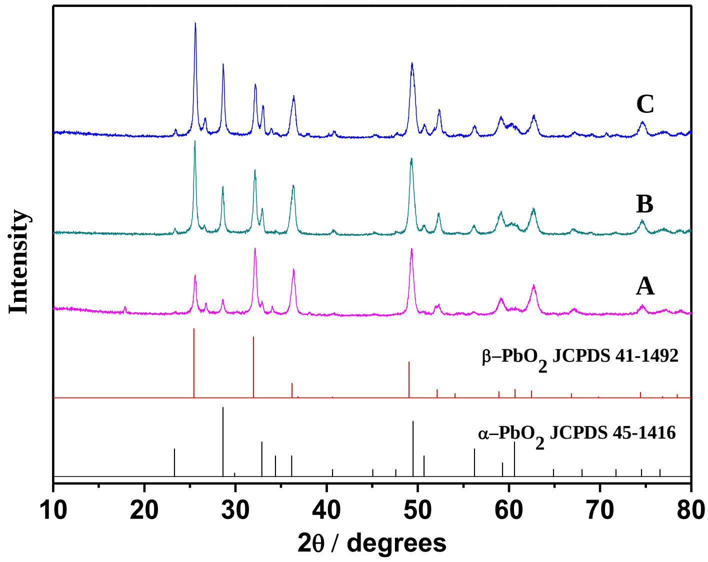

Figure 3. XRD patterns for the as-prepared thin films for PbO_2-20(A), PbO_2-70(B), and PbO_2-120(C).

The current efficiency for PbO_2-20, PbO_2-70 and PbO_2-120 formation was calculated by the following equation:

$$\eta=\frac{m_w}{m_t}=\frac{zFm_w}{MQA}$$

Where η represents the current efficiency, m_w was the mass difference of the subtract after deposition, m_t was the calculated deposition mass based on faradic formula, z was numbers of electrons involved in reaction, F for the Faradic constant (9.64853×10^4 C mol^{-1}), M for the relative molecular mass of PbO_2 (239.2 g mol^{-1}), Q for the total charge density (18 C cm^{-2}), A was the working area of the subtract (9 cm^{-2}). The calculated results showed that the current efficiency of PbO_2-20 thin film was 98.7% (22.04 mg cm^{-2}), while that of PbO_2-70 and PbO_2-120 was 85.2% (19.03 mg cm^{-2}) and 73.1% (17.06 mg cm^{-2}), respectively. This was consistent with the above observed deposition potentials in which more charge was consumed by oxygen evolution reaction.

Fig. 3 shows the XRD pattern of the as-prepared PbO_2 thin films. Based on the standard diffraction peaks (β-PbO_2 JCPDS 41-1492, α-PbO_2 JCPDS 45-1416), α and β-PbO_2 phase coexisted in those films. Meanwhile, the strong and sharp diffraction peaks were a sign of a good crystallinity. In addition, peak density for α-PbO_2 phase increased with the increasing of current density. Thus, as we expected, PbO_2 thin films with different structure and morphology were successfully fabricated with a facile electrodeposition approach by controlling the deposition current density.

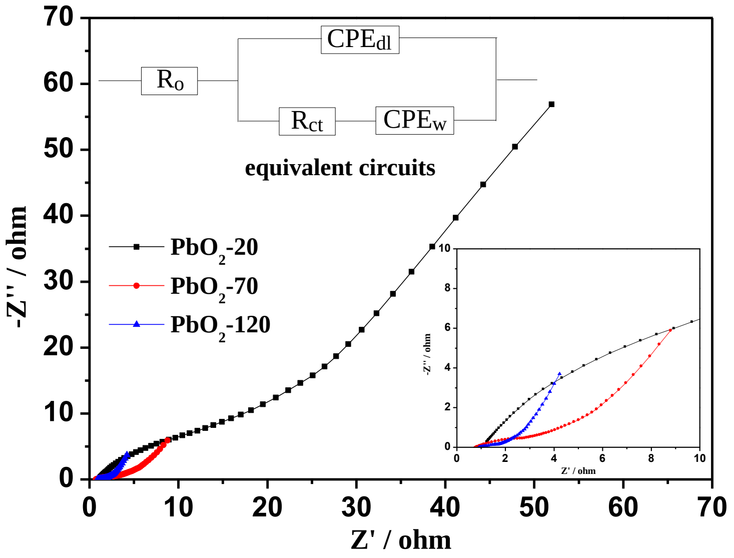

Figure 4. Nyquist plots of PbO_2 thin films in 1 M H_2SO_4 with 5 mV amplitude at 0.9 V; inset figures for the equivalent circuits and magnification of the high frequency region.

EIS as an effective method is broadly applied to probe the charge transfer kinetics of an electrochemical reaction[23]. It was determined in 1 M H_2SO_4 electrolyte and the Nyquist plots and equivalent circuit were presented in Fig.4. R_o stands for the ohmic resistance including uncompensated electrolyte resistance, contact resistance of the electrode and the internal resistance of the substrate. R_{ct} is charge transfer resistance related to the reduction of PbO_2 to $PbSO_4$. CPE_{dl} represents the double electric capacity that reflects the electrochemical active surface area, and CPE_w is for Warburg impedance. Due to the porous structure and high porosity, PbO_2-120 had a much higher CPE_{dl} values (1.11×10^{-3} F) compared to PbO_2-70 (4.2×10^{-4} F) and PbO_2-20 (8.04×10^{-5} F) thin films. In addition, it can be seen that PbO_2-120 thin films gave the smallest charge transfer resistance, and the specific R_{ct} of PbO_2-20, PbO_2-70 and PbO_2-120 thin films were 13.4, 1.83 and 0.65, respectively. The details information of parameters obtained from the equivalent circuit was compared in Table 1. Thus, the porosity structure with smaller particle size could enhance the electrochemical reaction rate by probably the improved ions transport toward the deep active layer. This was in consistent with the above results that porous structure was easily formed at high deposition current density.

Table 1. EIS fitting parameters from equivalent circuits for PbO_2 thin films

Sample	R_o	R_{ct}	CPE_{dl} (F)	CPE_w
PbO_2-20	1.46	13.4	8.04×10^{-5}	0.068
PbO_2-70	1.01	1.83	4.2×10^{-4}	0.14
PbO_2-120	1.02	0.65	1.11×10^{-3}	0.32

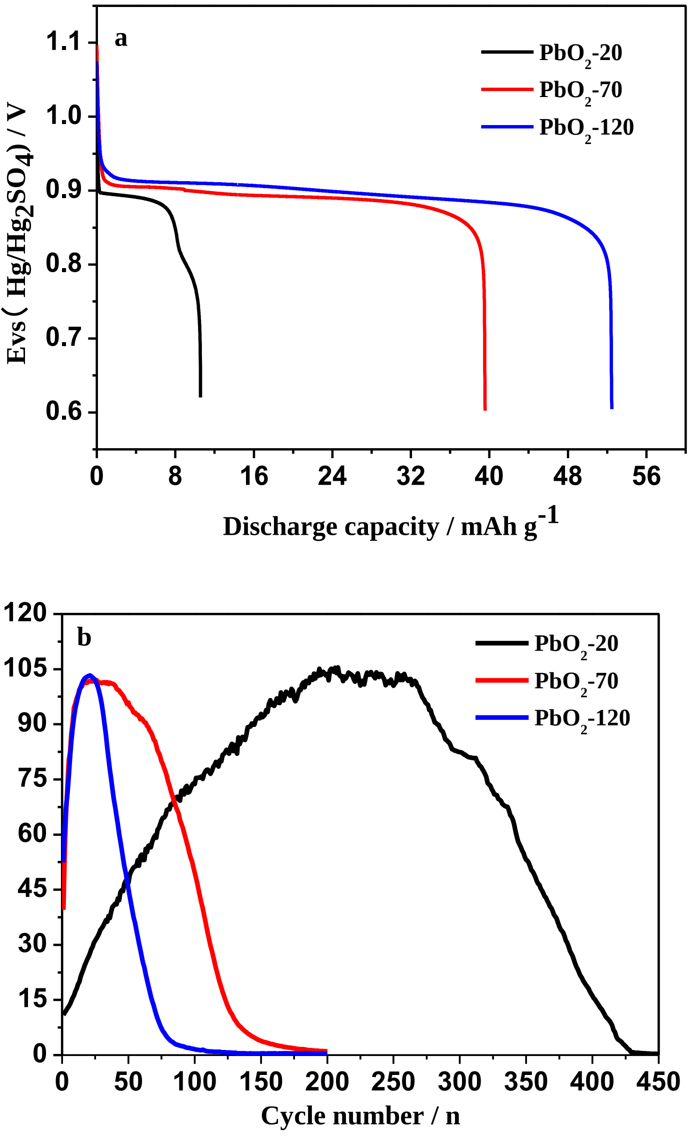

Figure 5. (a) The first discharge curves of PbO_2 thin films in 1 M H_2SO_4 solution at 250 mA g^{-1}, (b) cycling ability of discharge curves of PbO_2 thin films.

According to Pavlov et al[24], $PbSO_4$ exhibited a relative high electrochemical solubility during cycling in dilute acid solution (1 M H_2SO_4), thus the capacity and cycle life of these thin films with different surface microstructures was probed by GCD in 1 M H_2SO_4 at a discharge current density of 250 mA g^{-1} with cut-off potential of 0.6V. The initial discharge curves for the as-prepared thin films was shown in Fig. 5(a). Generally potential decrease was observed at the initial stage due to IR drop and internal impedance of the electrode, and then a steady-state discharge plateau was reached resulting from the reduction of PbO_2 to $PbSO_4$. In the end, the discharge potential was sharply decreased to the cut-off potential due to the serious concentration polarization caused by largely reduced diffusion ability of HSO_4^- ions. That was because discharge product of $PbSO_4$ gradually accumulated on the active sites to form a selective semipermeable membrane [25] that can block the diffusion of the larger diameter HSO_4^- ions towards the inside of active electrode material. Here, an initial discharge capacity of 52.5 mAh g^{-1} on PbO_2-120 thin film was obtained that was much higher than that of PbO_2-20(10.6 mAh g^{-1}) and PbO_2-70(39.6 mAh g^{-1}) thin films. The higher content of α-PbO_2 and the higher porosity and smaller particle size could account for the better capacity ability of initial PbO_2 thin films [26].

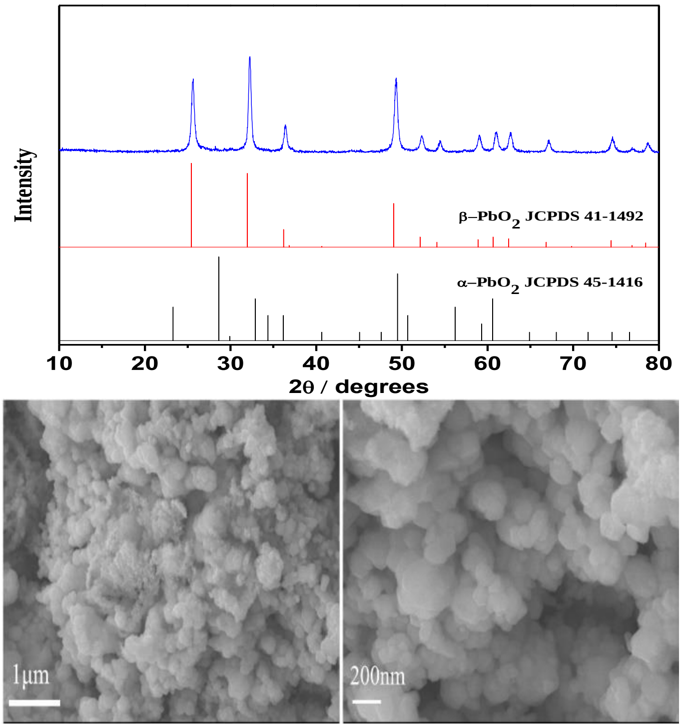

Figure 6. XRD patterns for the PbO_2-20 thin films after 200 cycles GCD measurements; FESEM images of PbO_2-20 thin films after 200 cycles GCD measurements.

However, when the GCD measurement was performed from 2nd to 450th cycles, an interesting result was obtained in which two different discharge behavior was observed for the films (Fig. 5b). A similar tendency was observed for PbO_2-70 and PbO_2-120 films in which the discharge capacity rapidly increased to a maximum value and then decreased largely by increasing the number of cycles. A maximum point around 100 mAh g^{-1} was observed at ca. 20th cycles, and the cycle ability for these films was less than 120 cycles. The reason was probably that the porous microstructure and smaller grain sizes were bad to adhere onto the substrate, thus the active material expansion-contraction will lead to the material falling off the substrate, and reddish brown suspension (PbO_2 particles) was observed in the electrolyte. While the discharge capacity was increased by increasing the cycle numbers on PbO_2-20 thin film until 200 cycles and a maximum capacity of 104.3 mAh g^{-1} was reached. After that, the capacity decreased gradually by cycling until 450 cycles at which the capacity was lost indicating its good properties capacity retention among these films. Thus, the porous structure of the PbO_2 thin film was not good for cycling charge-discharge ability.

Further investigation was focused on the PbO_2-20 thin film to acquire a proper explanation for the electrochemical behavior. The XRD pattern of PbO_2-20 thin film after 200 cycles GCD measurements was shown in Fig.6. Pure β-PbO_2 phase was observed in the film due to the irreversible transfer from α-PbO_2 to $PbSO_4$ as the oxidation product of $PbSO_4$ is β-PbO_2 [27]. Moreover, surface morphology change was observed compared with its initial state; microsphere morphology with small particle size was observed in comparison with the flat and dense surface morphology before cycling measurements (Fig.6). This change gradually happened due to the active materials expansion-contraction during charge/discharge cycles because of the molar volume difference between $PbSO_4$ (48.2cm^3 mol^{-1}) and PbO_2 (25.2cm^3 mol^{-1})[28]. So similar to the PbO_2-70 and PbO_2-120 samples, the discharge ability was gradually reduced once the porous structure was formed. Moreover, according to the PbO_2 active material gel-crystal theory proposed by Pavlov[29], intermediate product of $Pb(OH)_4$ was formed during the electrochemical oxidation process of $PbSO_4$ in sulfuric acid solution, and then gel zones of $PbO(OH)_2$ were formed with electron and proton conductivity beneficial for the absorption of HSO_4^- ion.

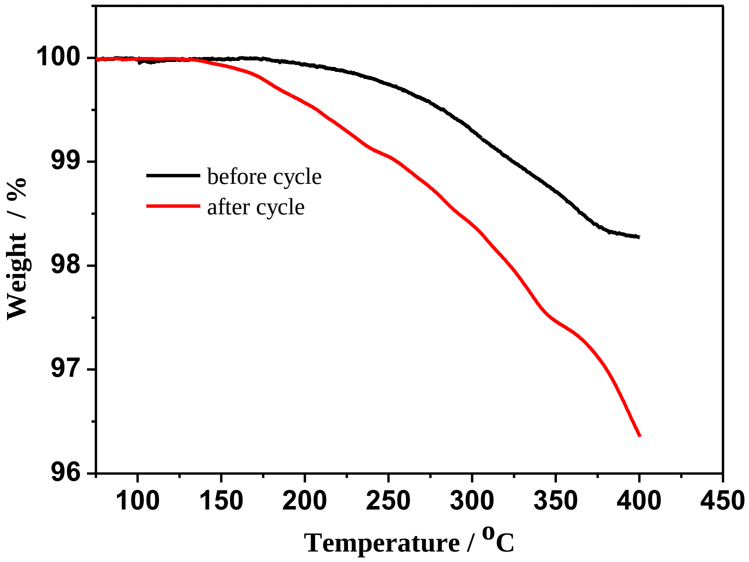

Figure 7. TGA curves of PbO_2-20 thin film before and after 200 cycles GCD measurement.

Therefore, it can be deduced that the content of gel zones $PbO(OH)_2$ was increased during cycling increase. Fig.7 showed the TGA curves for PbO_2-20 thin film before and after cycling measurements. Weight loss within the temperature range of 75 to 325 ^{o}C was due to the release of H_2O from gel zones of $PbO(OH)_2$ and evaporation of the water strongly bounded to the PbO_2 particles.

From 325 to 400°C temperature interval, weight loss was associated with the decomposition of β-PbO_2 to non-stoichiometric PbO_n(1<n<2)[19]. By comparing the weight loss of PbO_2-20 film before and after cycling measurements, it was confirmed that the content of gel-zone was increased from 1.7% to 3.7%.

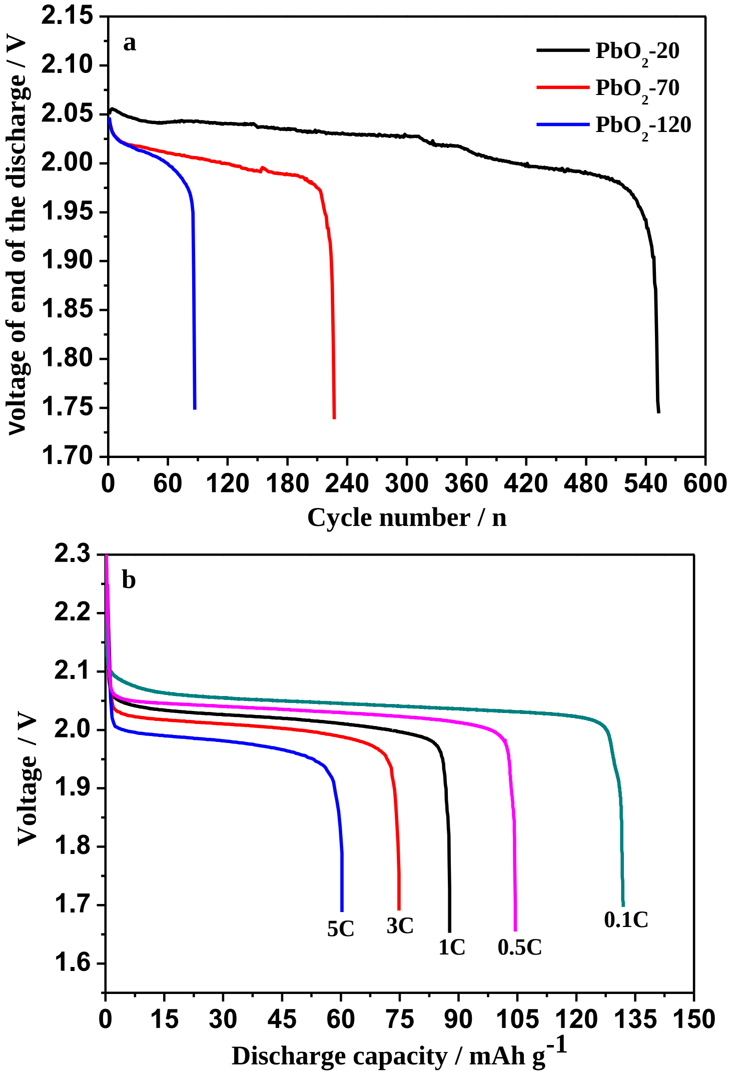

Figure 8. (a) The end of discharge potential versus cycle number of PbO_2 thin films in a laboratory battery at 1 C rate with 30% DOD; (b) rate performance of the battery employing PbO_2-20 thin film as positive plate with 100% DOD.

In order to evaluate the possible application of PbO_2 thin films in a lead acid battery, these thin films (after reaching their maximum capacity value during 100% DOD discharge cycling as done in Fig. 5b) were selected as positive plates, and tested in a laboratory battery. The cycle life measurement was carried out at 1C rate with 30% DOD, as shown in Fig.8a. The battery failure was considered as the end of discharge potential dropped below 1.75 V. It was observed that the end of discharge potential was approximately holding at 2 V before decreasing below 1.75V and the cycle number was 553 times for PbO_2-20. While it was 234 and 84 times for PbO_2-70 and PbO_2-120 thin films, respectively. After measurements, the reddish brown suspension was seen in the electrolyte, and then the active material could be washed off the substrate easily by distilled water. Thus, the failure of the thin film was resulting from softening and leaching of the active material.

After 200 cycles of 100% DOD discharge, the performance of PbO_2-20 thin film in the battery at different rates with cut-off potential of 1.75 V was presented in Fig.8b. The discharge rate has a significant influence on the discharge capacity. The thin film can deliver a capacity of 131.8 mAh g^{-1} at 0.1 C corresponding to 58.9% capacity of the theoretical value. The discharge capacity of 104.4 mAh g^{-1}, 87.7 mAh g^{-1} and 74.8 mAh g^{-1} was observed at 0.5C, 1C and 3C, respectively. Even at 5C, the film was still able to deliver a capacity of 60.2 mAh g^{-1}, and the potential of discharge plateau was about 1.95 V indicating a low internal resistance between the active material and active material/substrate interface. The discharge capacity and rate performance of the 2-D PbO_2 thin film in our experimental results were better than some literature reports. For example, a capacity not exceeding 40 mAh g^{-1} at 0.5C rate in 4.8 M solution during 100 charge/discharge cycles was reported on a PbO_2 thin film plate [30]. Due to the seriously sulfation phenomenon, the cycle life for a paste positive plate was around 225 times at 30% DOD with 0.25 C rate[31]. In a mini-tubular electrode a discharge capacity of 107 mAh g^{-1} could be reached during 210th cycles at 16.67 mA g^{-1} (about 0.12C rate)[32]. Furthermore, for comparison, electrochemical properties of PbO_2 thin films prepared by electrodepositing technique for energy storage and the as-prepared PbO_2-20 thin films that after activation cycles were listed in Table 2. Thus, after activation process, PbO_2 thin films electrodeposited at low current densities exhibited high capacity and rate performance.

Table 2 electrochemical properties of PbO_2 thin films in other researchers reports

Sample	Discharge condition	Electrolyte	Capacity	References
Ti/PbO_2	70mA g^{-1}	4.8M H_2SO_4	12.3mAh g^{-1}	[14]
Ti/PbO_2	900mA g^{-1}	1M H_2SO_4	20.8mAh g^{-1}	[15]
Ti/PbO_2	2A g^{-1}	0.1M KOH	49.5mAh g^{-1}	[33]
PbO_2-20	250mA g^{-1}	1M H_2SO_4	104.3mAh g^{-1}	This work
PbO_2-20	0.1C	5M H_2SO_4	131.8mAh g^{-1}	This work

4. CONCLUSION

In summary, PbO_2 thin films with different surface structures were successfully prepared by facilely controlling the electrodeposition current density. Though porous structure and smaller particle sizes can be gained at high deposition current density like PbO_2-70 and PbO_2-120 thin films that can facilitate the charge and reagent diffusion, poor cycle life was observed during GCD measurement. In the case of PbO_2-20 thin film, though the lowest initial discharge capacity was observed, a gradually increased discharge capacity was obtained until 200 cycles due to the change in microstructure surface and increased gel zone in active material, a phase transfer from α-PbO_2 to β-PbO_2 was observed in the film due to the irreversible transfer from α-PbO_2 to $PbSO_4$. The cycle life was 553 times during 30% DOD tests that was much higher than that of PbO_2-70 (84 times) and PbO_2-120 (234 times) thin films.

It was concluded that the porous structure of PbO_2 thin films was not preferred due to the bad cycling discharge ability.

ACKNOWLEDGEMENTS
The work is supported by the Priority Academic Program Development of Jiangsu Higher Education Institution.

References

1. A. Malhotra, B. Battke, M. Beuse, A. Stephan, T. Schmidt, *Renew.Sust.Energ.Rev.*, 56 (2016) 705.
2. J. Cho, S. Jeong, Y. Kim, Prog. *Energy Combust. Sci.*, 48 (2015) 84.
3. D. Cericola, M. Spahr, *J. Power Sources,* 324 (2016) 41.
4. M. Foudia, M. Matrakova, L. Zerroual, *J. Power Sources,* 279 (2015) 146.
5. A. Moncada, S. Piazza, C. Sunseri, R. Inguanta, *J. Power Sources*, 275 (2015) 181.
6. M.M. Hoque, M.A. Hannan, A. Mohamed, A. Ayob, *Renew.Sust.Energ.Rev.*, 75 (2017) 1363.
7. L.A. Yolshina, V.A. Yolshina, A.N. Yolshin, S.V. Plaksin, *J. Power Sources,* 278 (2015) 87.
8. X. Li, D. Pletcher, F.C. Walsh, *Chem. Soc. Rev.,* 40 (2011) 3879.
9. P.K. Shen, X.L. Wei, *Electrochim Acta.*, 48 (2003) 1743.
10. N. Yu, L. Gao, S. Zhao, Z. Wang, *Electrochim. Acta,* 54 (2009) 3835.
11. P. Perret, Z. Khani, T. Brousse, D. Bélanger, D. Guay, *Electrochim. Acta*, 56 (2011) 8122.
12. Y. Dan, H. Lin, X. Liu, H. Lu, J. Zhao, Z. Shi, Y. Guo, *Electrochim. Acta*, 83 (2012) 175.
13. Y. Dan, H. Lin, L. Chen, L. Zhang, J. Su, H. Yue, X. Cai, *RSC Adv.*, 5 (2015) 98983.
14. G. Darabizad, M.S. Rahmanifar, M.F. Mousavi, A. Pendashteh, *Mater. Chem. Phys.*, 156 (2015) 121.
15. W.L. Zhang, H.B. Lin, H.S. Kong, H.Y. Lu, Z. Yang, T.T. Liu, *Electrochim. Acta*, 139 (2014) 209.
16. A.B. Velichenko, D.V. Girenko, F.I. Danilov, *J. Electroanl. Chem.*, 405 (1996) 127.
17. D.R.P. Egan, C.T.J. Low, F.C. Walsh, *J. Power Sources*, 196 (2011) 5725.
18. D. Pech, T. Brousse, D. Bélanger, D. Guay, *Electrochim. Acta*, 54 (2009) 7382.
19. N. Chahmana, M. Matrakova, L. Zerroual, D. Pavlov, *J. Power Sources*, 191 (2009) 51.
20. Y.-q. Wang, B. Gu, W.-l. Xu, *J. Hazard Mater.*, 162 (2009) 1159.
21. P. Norouzi, T.M. Garakani, M.R. Ganjali, *Electrochim. Acta*, 77 (2012) 97.
22. N. Comisso, S. Cattarin, P. Guerriero, L. Mattarozzi, M. Musiani, E. Verlato, *Electrochim. Acta*, 200 (2016) 259.
23. M. Dimitrov, D. Pavlov, *J. Power Sources*, 93 (2001) 234.
24. D. Pavlov, A. Kirchev, M. Stoycheva, B. Monahov, *J. Power Sources*, 137 (2004) 288.
25. D. Pavlov, R. Popova, *Electrochim. Acta*, 15 (1970) 1483.
26. N. Fan, C. Sun, D. Kong, Y. Qian, *J. Power Sources*, 254 (2014) 323.
27. T. Chen, H. Huang, H. Ma, D. Kong, *Electrochimi. Acta*, 88 (2013).
28. M. Foudia, M. Matrakova, L. Zerroual, *J. Power Sources*, 207 (2012).
29. D. Pavlov, G. Petkova, M. Dimitrov, M. Shiomi, M. Tsubota, *J. Power Sources*, 87 (2000) 39-56.
30. [30] T. Chen, H. Ma, D. Kong, *Mater. Lett.*, 90 (2013) 103.
31. R. Marom, B. Ziv, A. Banerjee, B. Cahana, S. Luski, D. Aurbach, *J. Power Sources*, 296 (2015) 78.
32. M. Bervas, M. Perrin, S. Geniès, F. Mattera, *J. Power Sources*, 173 (2007) 570.
33. M.S.Soumya,G. Binitha, P. Praveen, K.R. Subramanian, Y.S. Lee, V.S. Nair, *J. Nanosci Nanotechnol.*, 15(2015) 703.

© 2018 The Authors. Published by ESG (www.electrochemsci.org). This article is an open access article distributed under the terms and conditions of the Creative Commons Attribution license (http://creativecommons.org/licenses/by/4.0/).